Available online at www.sciencedirect.com
ScienceDirect
Bioorganic & Medicinal Chemistry Letters 17 (2007) 6026–6030
Bioorganic & Medicinal Chemistry Letters

Solid-phase synthesis and thermal denaturation study of cyclic PNAs targeting the HIV-1 TAR RNA loop

Gregory Upert, Mohamed Mehiri, Audrey Di Giorgio, Roger Condom and Nadia Patino*

Laboratoire de Chimie des Molécules Bioactives et des Arômes (LCMBA), UMR UNSA-CNRS 6001, Université de Nice-Sophia Antipolis, 06108 Nice Cedex 2, France

Received 16 May 2007; revised 4 July 2007; accepted 5 July 2007
Available online 21 July 2007

Abstract—Cyclic PNAs targeting the HIV-1 TAR RNA loop have been synthesized following a convenient solid-phase strategy which allows on-resin cyclisation. UV-monitored thermal denaturation studies demonstrate that these cyclic PNAs are able to strongly interact with their TAR RNA target, very likely through the formation of a six-base pair stable complex, involving the TAR RNA loop.

The TAR RNA element of the HIV-1 genome (Fig. 1) is involved in essential steps of the viral life cycle, including transcription process,[1] reverse transcription and genomic RNA packaging.[2] HIV-1 transcriptional elongation is regulated via the formation of a ternary complex, involving the stem-loop TAR structure, the trans-activator viral protein Tat and cellular factors.[3] Both the stem and the apical loop of TAR are involved in this interaction. Therefore, ligands which interact with the TAR apical loop could disrupt the ternary complex, leading to abortive RNA synthesis.

Previously, the use of the SELEX approach (systematic evolution of ligands by exponential enrichment) allowed the identification of mini RNA hairpin aptamers which strongly interact with TAR to form 'kissing complexes', in part through loop–loop complementarity.[4] These aptamers contain the octameric sequence 5′-GTCCCAGA-3′, which includes the six-nucleotide sequence complementary to the TAR loop, flanked by a G and a A residues. Although these two residues are not directly involved in the loop–loop interaction, they are crucial for the formation of a stable kissing complex. Recently, it has also been shown that a chimeric LNA/DNA aptamer recognizes the TAR RNA stem-loop not only on the basis of the sequence complementarity, as classical antisense oligomers,

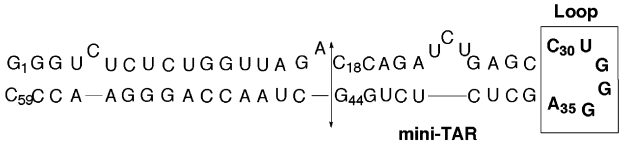

Figure 1. Structure of the 59 nt TAR RNA fragment (strain IIIb) and of the mini-TAR sequence used in this study.

but also on the basis of the tertiary structure of TAR. This particular mode of interaction leads to an increased selectivity of this LNA/DNA aptamer compared with the corresponding linear octameric 5′-GTCCCAGA-3′ antisense, demonstrating the advantage of aptameric structures over classical antisenses, for the design of highly specific TAR RNA ligands.[5] However, high mass aptamers permeate cellular membranes only upon complexation with cationic lipids and some of them are not stable in biological media, complicating thus their use as therapeutic agents.

In this context, we have elaborated biologically stable synthetic ligands of lower molecular weight than aptamers, liable to interact with TAR RNA through 'kissing-like' interaction. With this aim, we have designed constrained cyclic PNA derivatives **1a**–**c** containing the octameric PNA fragment 5′-GTCCCAGA-3′ (Fig. 2). PNAs are neutral nucleotide analogues resistant to nucleases. The N- and C-terminal extremities of the PNA oligomer backbone are, respectively, bound to a lysine and a glutamine residues, which are connected through a spacer. The glutamine residue has been used for syn-

Keywords: Cyclic PNA; On-resin cyclisation; HIV TAR RNA; Thermal denaturation studies; Kissing complex.
* Corresponding author. Tel.: +33 (0)4 92 07 61 46; fax: +33 (0)4 92 07 61 51; e-mail: patino@unice.fr

0960-894X/$ - see front matter © 2007 Elsevier Ltd. All rights reserved.
doi:10.1016/j.bmcl.2007.07.030

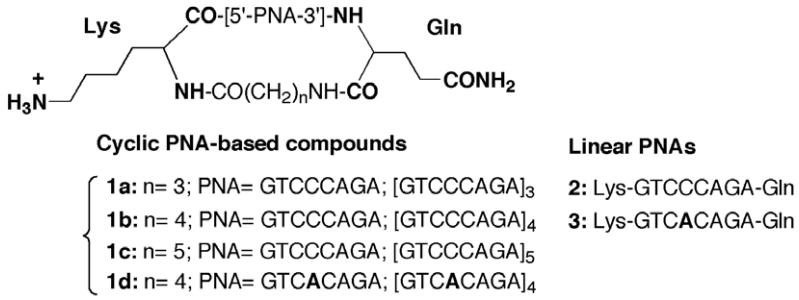

Figure 2. Structure of synthesized cyclic and linear PNA-based compounds. Residue in bold represents mismatched residues.

thetic purposes, as the resin-anchored residue (vide infra). The lysine residue has been introduced for conjugating **1a**–**c** to cell-penetrating moieties in view of subsequent cell-based assays. To evaluate the influence of the spacer length, three aminoacids ($n = 3, 4, 5$) have been selected on the basis of molecular modelling studies, starting from the 3D structure of the TAR/TAR* complex proposed by Tinoco et al. and applying geometric optimization.[8,7a]

To investigate the specificity of cyclic compounds **1a**–**c** to TAR, we have also studied the linear antisense PNA **2** incorporating the octameric consensus sequence, as well as a cyclic and a linear mismatched compounds, respectively, **1d** and **3** (Fig. 2).

In this paper, we report an efficient strategy for the solid-phase synthesis of cyclic PNA compounds. Interaction of compounds **1**–**3** with a mini-TAR RNA fragment (Fig. 1) has been studied by means of thermal denaturation experiments. For comparison, a RNA aptamer ($R06_{18}$), previously identified as a TAR RNA ligand through a SELEX procedure,[4] has been evaluated under the same conditions.

Only few papers in the literature report on the synthesis of cyclic PNA oligomers. In this context, due to inherent difficulties related to macrocyclisation and subsequent purification steps, simply achieving cyclic PNAs is still a challenging task. We have previously described the synthesis of cyclic PNAs following the 'Fully Protected Backbone' liquid-phase procedure (FPB), which consists of the preparation of a cyclic fullyprotected backbone precursor, containing many different and orthogonal protecting groups as there are different types of nucleic bases on the desired PNA. Then, a series of selective deprotection/coupling steps allows the insertion of the required nucleobases onto the cyclic framework.[6] However, a limitation of this method lies in the numerous acid and amino protecting groups required if the PNA contains more than three different types of nucleobases (at least eight orthogonal protecting groups). In this case, an alternative liquid-phase procedure, using both PNA and fully N-protected (aminoethylglycinamide) fragments, has been developed.[7] It offers the advantage, over the FPB strategy, of requiring less orthogonal protecting groups. However, unpredictable side reactions depending on the PNA sequence may occur, which makes this strategy difficult to generalize. Another interesting approach to synthesize cyclic PNA has been reported by Van Boom coworkers.[9] It comprises the solid-phase synthesis of linear N-terminal cysteine functionalized PNA-thioesters, followed by the intramolecular chemical ligation of the linear precursor upon release from the solid support. Recently, cyclic PNAs and cyclic PNA–DNA chimeras have been obtained using a new solid-phase approach,[10] which is based on the use of a Tentagel matrix functionalized with a linker containing two reactive groups, i.e., an amino group for the oligomer elongation and a phosphodiester group from which is performed the intramolecular cyclisation.

For our part, we have prepared cyclic compounds **1a**–**d** following an alternative and very attractive solid-phase strategy, via the on-resin head-to-tail cyclisation of the linear functionalized PNA precursors. This procedure, which has been applied for the synthesis of cyclopeptides,[11] cyclic aminoacid/PNA hybrids[12] and cyclic C-glycoside/aminoacid hybrids,[13] includes (i) the solid-support linkage to the glutamic acid side chain, (ii) the chain assembly of the linear sequence starting from the α-amino group of the resin-bound aminoacid, (iii) the head-to-tail cyclisation and (iv) the release of the cyclic compound from the support (Scheme 1).

The synthesis of compounds **1a**–**d** (Scheme 1) started by anchoring the *N*-α-Fmoc protected allyl glutamate residue (Fmoc-Glu-OAll) to the exposed amino group of the methylbenzylhydrilamide resin (MBHA-LL; loading capacity: 0.64 mmol/g) by means of HBTU preactivation, to obtain **4**. The resin was quarter-loaded to favour the intramolecular cyclisation step which is performed almost at the end of the synthesis. After capping of the unreacted amino groups with a mixture of Ac_2O/Pyridine/NMP, the Fmoc group on the glutamic acid residue was removed by 20% piperidine in NMP. Building of immobilized octamer PNA moieties **6** was then carried out progressively using the appropriate *N*-Boc (backbone) and *Z* (nucleobase) protected PNA monomer **5**, and applying the following three-step procedure: (i) preactivation of the selected PNA monomer using HBTU as activator and DIPEA as base, then on-resin condensation, (ii) capping of the unreacted amino groups, (iii) Boc cleavage with a 10% triisopropylsilane (TIS)/90% TFA solution. For each condensation step, the coupling efficiency was monitored using the Kaiser test. Extension of immobilized PNA **6** first with *N*α-Boc *N*ε-(2-Cl-Z) lysine residue, then with the convenient

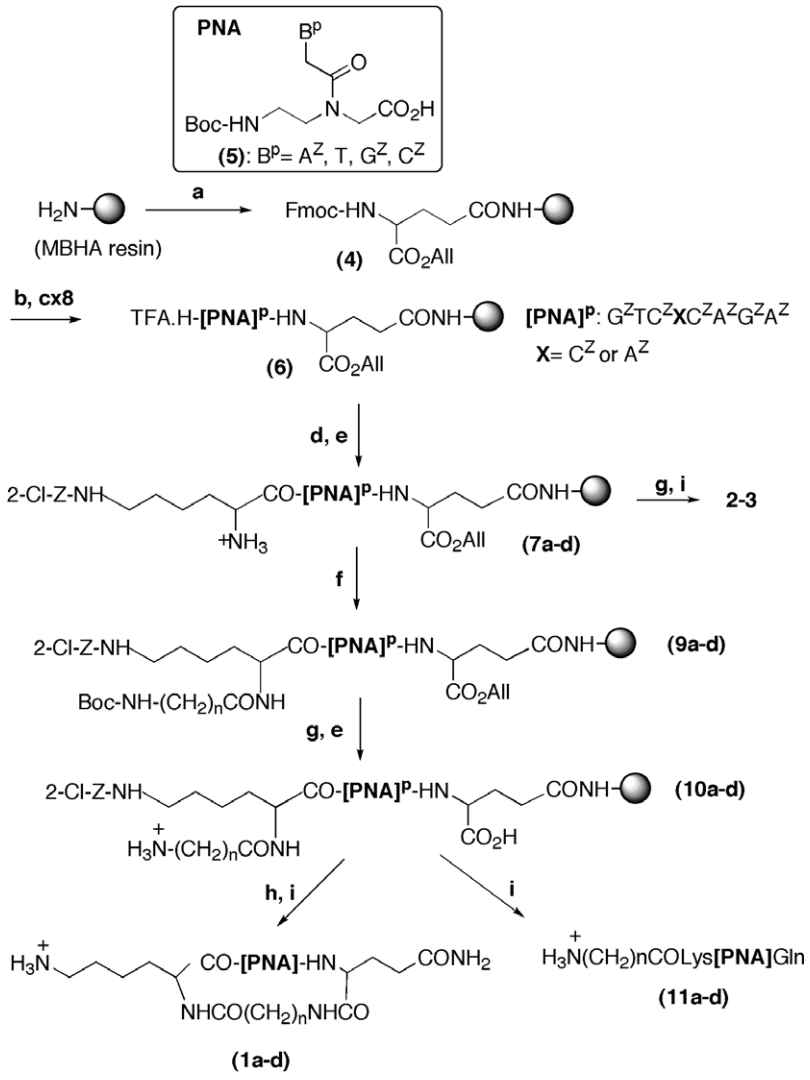

Scheme 1. Reagents and conditions: (a) i—Fmoc-Glu-OAll, HBTU, DIPEA, NMP; ii—Ac_2O/pyridine/NMP, 5 min; (b) 20% piperidine/NMP; (c) PNA elongation protocol: i—PNA monomer 5 (3.6 equiv), HBTU (3.5 equiv), DIPEA (17.5 equiv), NMP, 1 h; ii—Ac_2O/pyridine/NMP, 5 min; iii—10% TIS/TFA, two cycles of 15 min; (d) i—*N*α-Boc *N*ε-(2-Cl-Z)-Lys-OH (4 equiv), HBTU (4 equiv), DIPEA (20 equiv), NMP, 2 h; ii—Ac_2O/pyridine/NMP, 5 min; (e) TIS/TFA (9:1), two cycles of 15 min; (f) i—$BocNH(CH_2)_nCO_2H$ **5a**–**c** (*n* = 3, 4, 5) (4 equiv), HBTU (4 equiv), DIPEA (20 equiv), NMP, 2 h; ii—Ac_2O/pyridine/NMP, 5 min; (g) $Pd[P(Ph_3)]_4$ (0.5 equiv), DEA (30 equiv), NMP, 2 h; (h) PyAOP (5 equiv), DIPEA (10 equiv), NMP, 1 night; (i) TFMSA/TFA/TIS (1:1:8), 4 h.

N-Boc aminoacid spacer **8a**–**c**, was mediated following the same protocol, to provide immobilized functionalized PNA **9a**–**d**. Palladium-catalysed deprotection of the C-terminal allyl ester and subsequent Boc-removal from the N terminus extremity afforded the linear resin-bound precursors **10a**–**d**. At this stage, to check the purity of the crude linear products and to confirm their identity, a small aliquot of compounds **10a**–**d** was released from the support by acidolysis. After precipitation from cold diethyl ether and subsequent lyophylisation from water, HPLC and MALDI-TOF MS analyses revealed the presence of the linear compounds **11a**–**d** as the major products. Then, the on-resin cyclisation step was best performed by means of phosphonium salt-based reagents. Indeed, the use of PyBOP, PyAOP, or PyClock led, after simultaneous deprotection and cleavage from the resin with a TFMSA/TFA/TIS (1:8:1) solution, to compounds **1a**–**d** in about 30% yields, as shown by RP18 HPLC analyses of the crude reaction mixture (see Supporting information). The use of uronium salts reagents HATU or HCTU increased significantly the amount of by-products and gave only 11% of the desired product. An attempt was performed with 3-(diethoxyphosphoryloxy)-1,2,3-benzotriazin-4(3*H*)-one (DEPBT) as activator, as it has been reported to be more efficient for the cyclisation of peptides than uronium and phosphonium activators.[14] However, in our case, it gave unsatisfactory results (12% yield).

Linear PNAs **2**–**3** were prepared following the same procedure as for compounds **1a**–**d**. All compounds were purified by semi-preparative HPLC and the structures were confirmed by MALDI-TOF or ESI MS experiments.[15]

The binding to the miniTAR RNA fragment, of compounds **1a**–**d**, **2**–**3** and of the model aptamer $R06_{18}$, was studied by means of thermal denaturation experiments monitored by UV spectroscopy.[16] Melting

temperatures (T_m) were determined as the maximum of the first derivative of melting curves. The melting profiles obtained with mixtures of mini-TAR and individual tested compound displayed two transitions. The broad one at the highest temperature (T_m = 65.9 °C) results from the melting of the hairpin stem miniTAR, whereas the one at the lowest temperature reflects the melting of the PNA structures/miniTAR complex (Table 1).

The three cyclic compounds **1a**–**c** interact similarly with TAR, whereas the cyclic mismatch **1d** does not. This shows that the interaction between cyclic PNAs and TAR is sequence-specific. Besides, the linker length (n = 3, 4, 5) does not seem to have much influence since only slight T_m value differences are observed for the three PNA **1a**–**c**/TAR complexes ($\Delta T_m \approx 2$ °C).

To confirm that these complexes are bimolecular, the melting temperatures of the most stable complex (compound **1b**/miniTAR) were measured at different total concentrations. In the range of 8–2 μM, the T_m of the lowest transition decreases from 45.0 to 39.7 °C, as expected for a bimolecular complex,[17] whereas the T_m of the highest transition remains unchanged. Altogether, these results indicate that compound **1b** is able to interact with TAR RNA, very likely through the formation of a stable complex involving the two loops.

On the other hand, all cyclic **1a**–**c**/mini TAR complexes display a slightly increased thermal stability compared to the corresponding antisense **2**/miniTAR one ($\Delta T_m \approx 0.5$–3 °C) and a significantly increased stability comparatively to the $R06_{18}$/mini TAR ($\Delta T_m \approx$ 4.5–6.9 °C). Moreover, it must be noted that the mismatched cyclic compound **1d** does not bind to TAR RNA, in marked contrast to its corresponding linear derivative **3**. These results suggest that cyclic PNAs can be more specific TAR binders than classical antisenses, as it has been also shown in the case of LNA/DNA aptamers comparatively to LNA/DNA antisenses.[5] Surprisingly, the mismatched PNA **3** displays a higher T_m than the antisense PNA **2**. This observation has currently no explanation, and further experiments have to be performed to confirm and to understand these results. Nevertheless, the lysine and glutamine residues located at the 5′ and 3′ extremities of the PNA may be involved in the binding with TAR.

In summary, in an attempt to establish 'kissing-like' complexes with TAR RNA, we prepared cyclic PNA-based compounds following a convenient solid-phase strategy allowing on-resin cyclisation. Thermal denaturation studies revealed that these molecules strongly interact with their RNA target, likely through loop–loop interactions. Moreover, our results suggest that their mode of interaction with TAR is more specific than the one involving antisense PNA. Fluorescence anisotropy and electrophoretic mobility shift assays are currently under progress to assess the dissociation constant (K_d) of these complexes and to analyse their recognization process.

Subsequently, compounds **1a**–**c** will be conjugated to cell-penetrating moieties, in order to evaluate their ability to inhibit the HIV replication in cells.

Table 1. Melting temperatures of PNA structures/miniTAR complexes

N°	PNA structures	T_m (°C)
1a	$[GTCCCAGA]_3$	42.4 ± 0.3
1b	$[GTCCCAGA]_4$	43.4 ± 0.4
1c	$[GTCCCAGA]_5$	41.0 ± 0.3
1d	$[GTCACAGA]_4$	—
2	Lys-GTCCCAGA-Gln	40.5 ± 0.5
3	Lys-GTCACAGA-Gln	43.2 ± 0.1
$R06_{18}$	RNA aptamer	36.5 ± 0.3

Acknowledgments

We thank the 'Agence Nationale de Recherches sur le SIDA' (ANRS) and 'Fight Aids Monaco (F.A.M.)' for their grants. We are grateful to Jean-Jacques Toulmé and Carmelo Di Primo for providing us R06 RNA and for their useful advices, and to Rachel Philosoph from Luxembourg Industries for providing us PyClock coupling reagent.

Supplementary data

Supplementary data associated with this article can be found, in the online version, at doi:10.1016/j.bmcl.2007.07.030.

References and notes

1. (a) Roebuck, K. A.; Saifuddin, M. *Gene Expr.* **1999**, *8*, 67; (b) Jones, K. A.; Peterlin, B. M. *Annu. Rev. Biochem.* **1994**, *63*, 717; (c) Berkhout, B.; Jeang, K. T. *J. Virol.* **1989**, *63*, 5501.
2. (a) Harrich, D.; Hooker, C. W.; Parry, E. *J. Virol.* **2000**, *74*, 5639; (b) Harrich, D.; Hooker, B. *Rev. Med. Virol.* **2002**, *12*, 31; (c) Clever, J. L.; Mirandar, D.; Parslow, T. G. *J. Virol.* **2002**, *76*, 12381.
3. (a) Wei, P.; Garber, M. E.; Fang, S. M.; Fischer, W. H.; Jones, K. A. *Cell* **1998**, *92*, 451; (b) Fraldi, A.; Licciardo, P.; Majello, B.; Giordano, A.; Lania, L. J. *Cell Biochem.* **2001**, *36*, 247; (c) Richter, S.; Ping, Y. H.; Rana, T. M. *Proc. Natl Acad. Sci. U.S.A.* **2002**, *99*, 7928; (d) Richter, S.; Cao, H.; Rana, T. M. *Biochemistry* **2002**, *41*, 6391.
4. (a) Ducongé, F.; Toulmé, J. J. *RNA* **1999**, *5*, 1605; (b) Ducongé, F.; Di Primo, C.; Toulmé, J. J. *Biol. Chem.* **2000**, *275*, 21287.
5. (a) Darfeuille, F.; Reigadas, S.; Bo Hansen, J.; Orum, H.; Di Primo, C.; Toulmé, J. J. *Biochemistry* **2006**, *45*, 12076; (b) Lebars, I.; Richard, T.; Di Primo, C.; Toulmé, J. J. *Blood Cell. Mol. Dis.* **2007**, *38*, 204.
6. (a) Depecker, G.; Schwergold, C.; Di-Giorgio, C.; Patino, N.; Condom, R. *Tetrahedron Lett.* **2001**, *42*, 8303; (b) Schwergold, C.; Depecker, G.; Di-Giorgio, C.; Patino, N.; Jossinet, F.; Ehresmann, B.; Terreux, R.; Cabrol-Bass, D.; Condom, R. *Tetrahedron* **2002**, *58*, 5675; (c) Di Giorgio, C.; Depecker, G.; Schwergold, C.; Leroux, M. L.; Caldarelli, S.; Farese-Di Giorgio, A.; Patino, N.; Condom, R. *Recent Res. Devel. Nucleosides Nucleotides* **2003**, *1*, 81.
7. (a) Depecker, G.; Patino, N.; Di Giorgio, C.; Terreux, R.; Cabrol-Bass, D.; Bailly, C.; Aubertin, A. M.; Condom, R.

Org. Biomol. Chem. **2004**, *2*, 74; (b) Caldarelli, S.; Mehiri, M.; Di Giorgio, A.; Martin, A.; Hantz, O.; Zoulim, F.; Terreux, R.; Condom, R.; Patino, N. *Bioorg. Med. Chem. Lett.* **2005**, *13*, 5700.

8. (a) Comolli, L. R.; Pelton, J. G.; Tinoco, I. *Nucleic Acids Res.* **1998**, *26*, 4688; (b) Chang, K. Y.; Tinoco, I. *J. Mol. Biol.* **1997**, *269*; (c) Chang, K. Y.; Tinoco, I. *Proc. Natl. Acad. Sci. U.S.A.* **1994**, *91*, 8705.
9. De Koning, M. C.; Filippov, D. M.; Van der Marel, G. A.; Van Boom, J. H.; Overhand, M. *Tetrahedron Lett.* **2003**, *44*, 7597.
10. Moggio, L.; De Napoli, L.; Di Blasio, B.; Di Fabio, G.; D'Onofrio, J.; Montesarchio, D.; Messere, A. *Org. Lett.* **2006**, *8*, 2015.
11. (a) Kates, S. A.; Solé, N. A.; Johnson, C. R.; Hudson, D.; Barany, G.; Albericio, F. *Tetrahedron Lett.* **1993**, *34*, 1549; (b) Alsina, J.; Rabanal, F.; Giralt, E.; Albericio, F. *Tetrahedron Lett.* **1994**, *35*, 9633; (c) Cabrele, C.; Langer, M.; Beck-Sickinger, A. G. *J. Org. Chem.* **1999**, *64*, 4353; (d) Yan, L. Z.; Edwards, P.; Flora, D.; Mayer, J. P. *Tetrahedron Lett.* **2004**, *45*, 923; (e) Gonçalves, M.; Estieu-Gionnet, K.; Laïn, G.; Bayle, M.; Betz, N.; Déléris, G. *Tetrahedron* **2005**, *61*, 7789.
12. Planas, M.; Bardaji, E.; Barany, G. *Tetrahedron Lett.* **2000**, *41*, 4097.
13. Katajisto, J.; Lönnberg, H. *Eur. J. Org. Chem.* **2005**, 3518.
14. Ye, Y. H.; Li, H.; Jiang, X. *Biopolymers* **2005**, *80*, 172.
15. HPLC method: solvent A: H_2O/0.1% TFA, solvent B: CH_3CN/0.1% TFA; 7 min 100% A then gradient from 100% A to 50/50 A/B in 45 min, T = 55°C. For compound **1a**: HPLC t_R = 19.7 min, MALDI-TOF MS calcd for $C_{100}H_{132}N_{52}O_{27}$: 2491.0557, found *m/z* = 2492.2694; for compound **1b**: HPLC t_R = 20.0 min, MALDI-TOF MS calcd for $C_{101}H_{134}N_{52}O_{27}$: *m/z* = 2507.0713, found *m/z* = 2508.4966; For compound **1c**: HPLC t_R = 20.3 min, MALDI-TOF MS calcd for $C_{102}H_{136}N_{52}O_{27}$: *m/z* = 2521.0869, found *m/z* = 2522.4072. For compound **1d**: HPLC t_R = 20.4 min, ESI MS calcd for $C_{103}H_{135}N_{53}O_{26}$: $[M+H]^+$: 2531.1, $[M+3H]^+/3$: 844.7, found $[M+Na]^+$: 2555.2, $[M+3H]^+/3$: 845.2; For compound **2**: HPLC t_R = 17.9 min, ESI MS calcd for $C_{97}H_{128}N_{50}O_{27}$: $[M+2H]^+/2$: 1214.0, found $[M+2H]^+/2$: 1214.4; For compound **3**: HPLC t_R = 18.0 min, ESI MS calcd for $C_{98}H_{128}N_{52}O_{26}$: $[M+H]^+$: 2450.1, $[M+2H]^+/2$: 1226.0, $[M+3H]^+/3$: 817.7, found $[M+H]^+$: 2451.2, $[M+2H]^+/2$: 1226.4, $[M+3H]^+/3$: 818.0.
16. *Thermal denaturation*. Individual compounds and mini-TAR (2 μM each) were preincubated for 1 h at 25 °C in 500 μL of a 20 mM sodium cacodylate buffer, pH 7.3, containing 140 mM potassium chloride, 20 mM sodium chloride and 0.3 mM magnesium chloride (R buffer). The thermal denaturation was generated by increasing the temperature from 5 to 90°C, at 0.4°C/min, and was followed by UV absorption at 260 nm on an Varian Cary 300 spectrophotometer. The melting temperature (T_m) was determined as the maximum of the first derivative of the melting curve.
17. Puglisi, J. D.; Tinoco, I. *Methods Enzymol.* **1989**, *180*, 304.